*ISSN 2522-9400* **European Modern Studies Journal** *Vol 7 No 2*
*available at www.journal-ems.com*
*DOI: 10.59573/emsj.7(2).2023.20*

# Investigation of the Optical Properties and Bandgap Energy of CdCuS Using the Successive Ionic Layer Adsorption Reaction (SILAR) Method of Thin Film Deposition

Marius O. Eji, Andrew C. Aniagboso, Tobias O. Ayogu, and J. I. Ezema
Department of Physics and Astronomy, University of Nigeria, Nsukka, Nigeria

**Abstract.** The optical properties and bandgap energy of Cadmium Copper Sulfide (CdCuS) were investigated using the Successive Ionic Layer Adsorption Reaction (SILAR) method of thin film deposition. The experiment was conducted at a temperature 333k (60°C), and at three different cycles: 20, 30 and 40 respectively. UV-vis spectrophotometer was used in the characterization, and Origin Lab software was used in the computation and graph plotting. From the result obtained, the maximum transmittance and reflectance occur at the visible and infra-red regions in the electromagnetic spectrum. Also, the bandgap energy for 20, 30, and 40 cycles are approximately: 1.26eV, 1.38eV, and 1.57eV respectively. The analysis of the bandgap energy strongly suggests that increase in the bandgap value decreases the electrical conductivity, hence the substrate deposited at 40 cycles has the least electrical conductivity. Further analysis of the bandgap energy revealed that CdCuS deposited by SILAR method has prominent applications in optical devices and solar cells.

**Key words:** Bandgap, Optical, SILAR, CdCuS, Deposition, Thin Films

## Introduction

The technology of thin film has attracted significant attention over the years due to its potential application in fabricating Nano devices. Thin film deposition is the act of depositing chemical substances on the treated substrates to change their physical and chemical properties. Also, thin film deposition is the process of creating and depositing thin film coating onto substrate materials. Different materials such as; metal oxides and compounds can be used to do the depositions. The materials deposited through this method have promising applications in optical devices, electronics devices, solar energy devices, sensing devices and biomedical devices.

Thin film materials can be deposited by different methods such as: Successive Ionic Layer Adsorption Reaction (SILAR) method, Chemical Bath Deposition (CBD) method, Chemical Vapor Deposition (CVP) method and many more. The deposition of thin film materials using the successive ionic layer adsorption reaction (SILAR) method is mostly preferred because, it is simple, cost less, and also does not require much time (Sakapal, Mane, & Lokhande, 2001). SILAR method is considered as the simplest technique for material synthesis owning to its flexibility, large-area fabrication, and low processing temperature (Patwary, 2022). It is simple, inexpensive, and works best for large area deposition (Pathan & Lokhande, 2004). More so, SILAR method prevents substrates' oxidation and corrosion due to its low processing temperature. Changes in parameters such as; PH value, temperature, concentration of solution, and thickness affect the thin film amplification (Tasdemirci, 2019). In the SILAR method, two precursors solutions are prepared where substrates are immersed, and washed with water that is in between to remove non-adhesion thin film. Thus, one SILAR cycle consists of adsorption of the cations precursors, rinsing with water, adsorption of anions precursors, followed by reaction and another rinsing (Sakapal, Mane, & Lokhande, 2001).

In the optical characterization, absorbance, transmittance and reflectance are the important parameters in material characterization. Absorbance helps in calculating the actual

photon energy. The sum of the absorbance ($a_{ab}$), transmittance (T), and Reflectance (R) yields unity (Kodigala, 2010).

$$a_{ab} + T + R = 1 \quad (1)$$

When the reflectance and transmittance are known, one can determine the transmittance from the absorbance using the relation

$$T = 10^{-A} \quad (2)$$

Where (T) is the transmittance and (A) is the Absorbance.

According to Nadeem and Ahmed, (2000), the reflectance (R) is related to the refractive index (n) as;

$$R = \frac{(n-1)^2}{(n+1)^2} \quad (3)$$

Where (n) is the refractive index. We can rearrange equation (3) to have

$$n = \frac{1+\sqrt{R}}{1-\sqrt{R}} \quad (4)$$

The absorption coefficient $\alpha(hv)$ and the photon energy $E(hv)$ are related as (Nadeem & Ahmed, 2000);

$$\alpha(hv) = A(hv - E_g)^n \quad (5)$$

Where the absorption coefficient $\alpha(hv)$ is given as (Nadeem & Ahmed, 2000)

$$\alpha(hv) = 2.303 \frac{A}{t} \quad (6)$$

(A) is the admittance, ($E_g$) is the bandgap energy and (t) is the thickness of the thin film deposited.

The relationship between the admittance (A) and the wavelength of radiation shows that

$$A = \alpha(hv) * \lambda \quad (7)$$

Equation (7) proves that one can determine the absorption coefficient when the thickness of the film is not given. From equation (5), we have that for direct transition, the integer (n) in the index is n= ½. If we square both sides of equation (5), we have;

$$\alpha(hv)^2 = A^2 (hv - E_g)^{2n} \quad (8)$$

So that if n=1/2, then equation (8) becomes,

$$\alpha(hv)^2 = A^2((hv - E_g) \quad (9)$$

The factor $(hv)$ is called the photon energy. The plot of $\alpha(hv)^2$ against the photon energy shows that at the point $\alpha(hv)^2=0$, the bandgap energy ($E_g$) equals the photon energy, i.e

$$hv = E_g\ (eV) \quad (10)$$

Where the photon energy $(hv)$ is given as ;

$$hv = 1240/\lambda \text{ in } (eV) \quad (11)$$

This means that we can obtain the bandgap energy by extrapolation even if there is no point where the line intersects the photon-energy axis. The wavelength (λ) is given in nanometer (nm) and energy in electron volts (eV).

*Bandgap energy:* The bandgap energy is an energy range where no electron can exist in an atom. It is the energy difference between the top of the valence band and the bottom of the conduction band in insulators and semiconductors. This is the predominant factor in determining the electrical conductivity of a solid. The higher the bandgap the lower the electrical conductivity. Hence, insulators have the highest bandgap followed by semiconductors, while conductors have little or none band-gap.

**Methodology**

The apparatus provided for the deposition were salt sample labelled: sample **(A)**, (**B**), (**C**), (**D**) and (**E**), 100ml beakers, 10ml syringe, distilled water, electronic scale, measuring cylinder, filter paper, pre-treated 2*6 $cm^2$ glass slides, stopwatch, spatula and stirring rod.

Sample (**A**)-CADMIUM NITRATE TETRAHYDRATE [$C_dN_2O_6.4H_2O$], molecular weight ($M_w$) =308.47g/mol, Sample (**B**)-COPPER NITRATE [$C_U(NO_3)_2.3H_2O$] of molecular weight ($M_w$) = 241.60g/mol, Sample (**C**)-THIOUREA [$NH_2CSNH_2$) of molecular weight ($M_w$) =76.12g/mol, Sample (**D**)-Ammonia ($NH_3$), molecular weight ($M_w$) =17g/mol, and Sample (**E**)-SODIUM-HYDROXIDE (NaOH), molecular weight ($M_w$) = 40g/mol

The general molarity relation is $g= \frac{MVM_w}{100}$ (12)

Where g is the mass of the sample in grams, M is the mole of interest to be prepared, V is the volume of interest to be prepared, $M_w$ is the molecular weight of the sample to be prepared.

The mass of the sample, A, B, C and E, were calculated using equation (12), and determined using the weighing scale. 0.025 M of 100ml of samples (A) and (B) each were prepared by weighing out 0.77g of sample A, and weighing out 0.604g of sample B, as calculated using equation (12). In a separate container, these two samples were mixed with 100ml of distilled water each to dissolve the sample in a liquid phase. The stirrer was used to hasten the reaction. Thereafter, 1:1 ratio of samples A and B were mixed and this gives the cationic precursor. The ratio was mixed 30ml each into a different container. Also, for the anionic precursor, 0.19g of salt sample (C) was weighed and mixed with 100ml of distilled water in a separate container. Sample (D) was in the liquid phase already, and it was diluted with distilled water. 6ml of sample (D) and 44ml of the distilled water were mixed to obtain the 50ml of the sample (D). Again, 0.1g of sample (E) was weighed and mixed with 50ml of distilled water. The mixture was stirred and put in a separate container.

Solutions (C) and (D) were mixed in the ratio 1:1 and this corresponded to 30ml volume of each. 20ml of the solution (D) and (C) was mixed with (E) and the mixture was stirred. This gives the anionic precursor. The cationic and anionic precursors were put in the beakers labelled (J) and (L) respectively. Beakers (K) and (M) were also filled with 80ml of distilled water in each. The placement of these beakers are shown in Figure 1. In Figure 1, Beaker (J), Beaker (K), Beaker (L), and Beaker (M) are placed horizontally on a water bath which maintained a steady temperature of 333K (60℃) throughout the deposition time. The pre-treated substrate was immersed in the cationic precursor that is contained in the beaker (J) and was stirred for 20 seconds with a stirrer. Immediately, the substrate was rinsed in the distilled water contained in the beaker (K) for 5 seconds to remove non-adhesion thin films. Also, the substrate was immersed in the anionic precursor solution contained in the beaker (L) for 20 seconds and then rinsed in the fourth beaker (M) that contained distilled water for another 5 seconds to remove non-adhesion thin films as well. These four steps make one complete cycle, and the whole processes were repeated for 20, 30 and 40 cycles using three pre-treated substrates. The deposited substrates were allowed to dry in the air after the deposition.

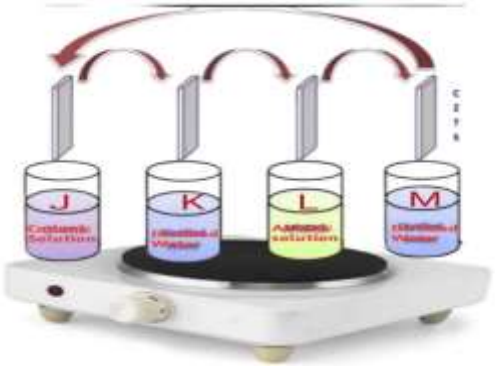


**Figure 1: Practical Set up**

## Results and Discussion

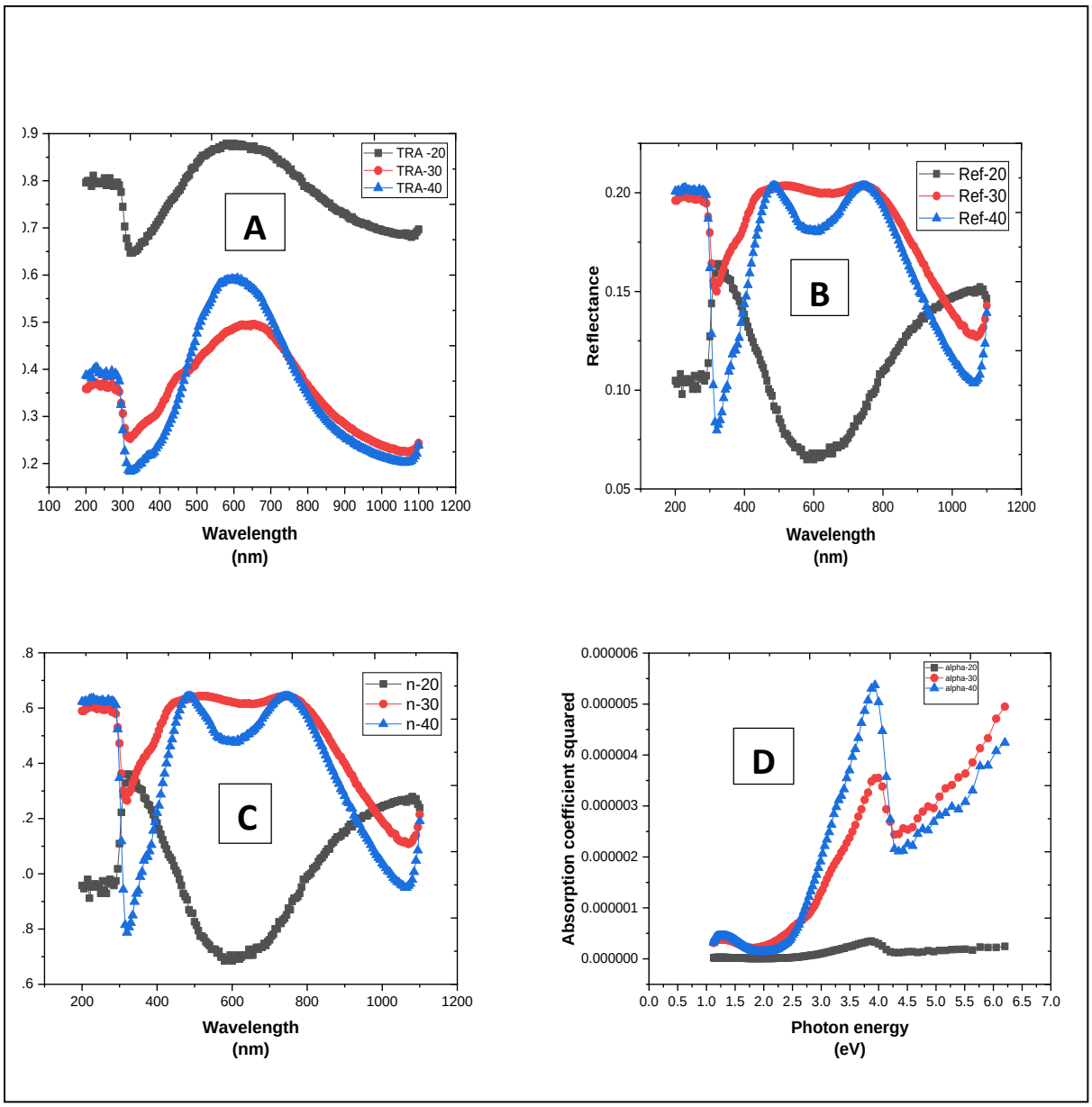


**Figure 2: (i) A, B and C are the plots of transmittance, reflectance and refractive index against wavelength (ii) D is the plot of absorption coefficient square against the photon energy**

The graphs in Figure 2 are the summary of the result obtained from the experimental investigation of the optical properties of CdCuS using SILAR technique. The substrates deposited were characterized using UV-VIS spectrophotometer. Using equation (2), the transmittance for the different cycles were calculated. Also, equation 1, 4, 6 and 9, were used to calculate the reflectance, refractive index, absorption coefficient and the photon energy.

Figure 2A is the graph that shows the variations of the transmittance for different cycles against wavelength. The symbols (TRA-20), (TRA-30), and (TRA-40) are the transmittance curves for 20, 30 and 40 cycles respectively. The graph indicates that the radiations have the highest transmittance during the 20-cycles, followed by the 40 cycles and then the 30 cycles.

Though, the substrates were deposited at the same steady temperature, the graph proves that the transmittance and the number of cycles is not a linear relationship. The peak transmittance wavelength for the three curves is in the range 500-670nm. Mohammad (2018), deposited nanocrystalline Copper-Cadmium-Sulfide ($Cu_xCd_{1-x}S$) using chemical bath deposition method, his result obtained from UV-vis spectrophotometer shows that optical transmittance wavelength is in the range 300-1100nm. From Figure 2A, the peak transmittance for 20 cycles corresponds to 580nm wavelength, while 30 and 40 cycles correspond to 655nm and 610nm. In the electromagnetic spectrum chart, the visible region falls in the wavelength range 400nm-700nm, this implies that the values of the transmittance wavelength correspond to the visible region in the electromagnetic spectrum. High transmittance occurs in the visible and close to Infra-red (IR) regions (Solai, Usha, & Prasath, 2023). Shaikh, Satpute, and Gadde (2023), synthesized CdS thin film using chemical bath deposition method at different deposition temperatures in the range 50-80℃. Optical spectra of their work revealed that at the temperature 50-80℃, the transmittance is up to 70-85%.

Figure 2B is the plot of the reflectance against the wavelength. This is consistent with the variation of the transmittance-wavelength graph, and the peak reflectance equally appears in the visible region in the electromagnetic spectrum for the three cycles. Eze and Eya (2012) works on the chemical bath deposition of CdS-PbS thin films, their result indicates that the peak reflectance of these films is within the visible region. Figure 2C is the graph that shows the variations of the refractive index against the wavelength for the different cycles. The curves are labelled n-20, n-30, and n-40 for the refractive index against wavelength for the 20, 30 and 40 cycles respectively. The refractive index is the parameter that describes how radiations are bent when they penetrate a material. The analysis of the refractive index near the visible and infrared regions shows that the peak refractive index for the 20 cycles is lower than that of the 40 cycles, while the 30 cycles have the least refractive index. Investigation of the optical properties of CdMnS using electrodeposition method shows that optical conductivity, refractive index, absorption co-efficient, and absorbance are affected by deposition voltage (Nwori et al., 2022). Figure 2D is the plot of the absorption coefficient square against the photon energy for the 20, 30 and 40 cycles. The curves alpha-20, alpha-30 and alpha-40 are the graphs of the absorption coefficient square versus photon energy for 20, 30 and 40 cycles respectively. The bandgap energies for the three curves were obtained by extrapolating the curves in the origin lab software using a straight line. The results are shown in the table below;

**Table 1**

| Number of cycles | Band gap energy |
|---|---|
| 20 | 1.26eV |
| 30 | 1.38eV |
| 40 | 1.57eV |

Table 1 shows the bandgap energies obtained for different cycles. In this table, there is a direct relationship between the number of the cycles and the bandgap energy. This energy increases as the number of cycles increases, which result in an increase in the deposition time. As the time of the deposition increases, the thickness of the materials increases, this leads to the decrease in the bandgap edge and increase in the bandgap energy. Devi and Singh (2020) studied the optical properties of CdS and CdCuS using chemical bath deposition, their result shows that the bandgap energy of CdS and CdCuS are 1.74eV and 1.77eV respectively. Gunaskaran, and Akumaran (2020) noted that the bandgap energy of CdS, CdNiS, CdTiS, and CdZnS deposited using SILAR method are 3.7191eV, 3.8195eV, 3.8490eV, and 3.9651eV respectively. CdMnS fabricated using chemical bath deposition has

moderate transmittance in the VIS-NIR regions, and bandgap energy in the range 1.4-1.65eV (Oriaku, Ezema, & Osuwa, 2008). The bandgap energy of $Cu_xCd_{1-x}S$ deposited using chemical bath deposition is 3.77eV at x=0.1 (Mohammad, 2018). As the $Cu^{2+}$ content increases in chemical bath solution, band gap energy also increases. Desale et al (2011) revealed that the bandgap energy of CdS is 2.5eV. The addition of copper (Cu) as an impurity in the deposition of CdCuS lowers the band-gap energy, as observed from our experimental result in Table 1. The bandgap energy is the predominant factor used to estimate the electrical conductivity. The result of this study shows that the substrate deposited at 20 cycles has high electrical conductivity, followed by the substrate deposited at 30 cycles, while the substrate deposited at 40 cycles has less conductivity. More so, the analysis of the energy bandgap for the deposited substrates shows that CdCuS deposited by SILAR method has prominent applications in optical devices and solar cells.

## Conclusion

SILAR method was used to investigate the optical properties and bandgap energy of CdCuS. The deposition was carried out at 333k (60℃) temperature and at three different cycles (20, 30 and 40). The analysis of our experimental result indicates that the peak transmittance and reflectance occur at visible and infra-red regions in the electromagnetic spectrum. Also, the bandgap energy increases as the deposition time increases. The electrical conductivity is dependent on the bandgap energy, increase in bandgap energy decreases the electrical conductivity and verse versa. Hence, the substrate deposited at 20 cycles is a good conductor of electricity, followed by the substrate deposited at 30 cycles, while the substrate deposited at 40 cycles has less conductivity. Further analysis of the result proves that CdCuS synthesized by the SILAR method is a potential material for the fabrication of optical devices and solar cells owing to its small bandgap values.

## Recommendation

We investigated the optical properties of CdCuS by the SILAR method, but scientific knowledge is cumulative. In this regard, there are needs to investigate the optical properties of CdCuS using other methods of material deposition such as; electrochemical deposition, chemical vapor deposition, e.t.c. Also, further research should be conducted on CdTiS, CdNiS, CdMnS, CdZnS e.t.c using both SILAR and other methods of material deposition.

## References

Desale, J. D., Shaik, S., Siddqui, F., Ghosh, A., Birajdar, R., Ghule, A.V., & Sharm, R. (2011). Effect of annealing on structural and optoelectronic properties of CdS thin films by Silar method. *Adv. Appl. Sci. Res., 4*, 417-425.

Devi, I.R., & Singh, L.R. (2020). Study of optical properties of CdS and Cu-doped CdS thin fabricated by chemical bath deposition technique. *International Journal for Innovative Research in Multidisciplinary fields, 6*(3).

Eze, F.C., & Eya, D.D.O. (2012). Chemical bath deposition and characterization of CdS-PbS thin films. *Nigerian Journal of Physics, 23*(1), 21-34.

Gunaskaran, M., & Akumaran, P.S. (2020). Structural and optical properties of silar deposited CdS, Ni, Ti, and Zn DOPED CdS thin films. *International Journal of Thin Film Science and Technology, 9*(3).

Mohammed, J.F. (2018). Structural and Optical properties of nanocrystalline $Cu_xCd_{1-x}S$ thin film deposited by chemical bath deposition technique. *Journal of Nano-Oxide Glasses, 10*(1), 27-2.

Nadeem, M.Y. & Ahmed, W. (2000). Optical properties of ZnS thin film. *Turkish Journal of Physics, 24*(6), 5.

Nwori, A., Okoli, N., Okeke, A.N., Ottih, I.E., & Ezenweke, L. (2022). Optical properties of electrodeposited CdMnS thin film semiconductor alloys for optoelectronics application: Effect of deposition potential. *Journal of Nano and Material Science Research, 2*, 58-57.

Oriaku, C.I., Ezema, F.I., & Osuwa, J.C. (2008). Fabrication and optical constants of CdMnS ternary thin films deposited by chemical bath. *Pacific Journal of Science and Technology*, *10*(1).

Pathan, H.M., & Lokhande, C. (2004). Deposition of metal chalcogenide thin films by successive ionic layer adsorption and reaction (silar) method. *Bullentin of Material Science, 282*, 85-111.

Patwary. (2022). Thin films processed by SILAR method. *Intechopen*.

Kodigala, S. (2010). Optial properties of I-II-VI compounds. *Thin Films and Nanostructures, 35*, 197-317.

Sakapal, B.R., Mane, R.S, & Lokhande, C.D. (2001). Successive ionic layer adsorption and reaction (SILAR) method of the deposition of large area (210$cm^2$) tin disulfide ($SnS_2$) thin films. *Materials Bulletins, 35*, 2027-2035.

Shaikh, A.Z., Satpute, A.S., & Gadde, J.R. (2023). Infuence of chemical bath deposition temperature on Cadmium Sulphide thin film and photosensor application. *ES Materials and Manufacturing*.

Solai, S., Usha, K.S., & Prasath, G. V. (2023). Ammonia gas sensing performance of Co/Ni co-doped CdS thin films by chemical bath deposition. *Journal of Materials Science: Materials in Electronics, 1*, 34.

Tasdemirci. (2019). Effect of different thickness and solution concentration on CuS thin film grown by silar method. *Journal of Scientific Perspective, 3*(3).